MG132 protects against lung injury following brain death in rats

HUIJUAN SHI[1-4], DONGJING YANG[1-3], ZHONGKUN HUO[1-3], YUEXIA LI[1-4], WENZHI GUO[1-3] and SHUIJUN ZHANG[1-3]

[1]Department of Hepatobiliary and Pancreatic Surgery, The First Affiliated Hospital of Zhengzhou University; [2]Henan Open and Key Laboratory for Hepatobiliary & Pancreatic Surgery and Digestive Organ Transplantation, The First Affiliated Hospital of Zhengzhou University; [3]Zhengzhou Key Laboratory for Hepatobiliary & Pancreatic Diseases and Organ Transplantation; [4]Department of Intensive Care Unit, The First Affiliated Hospital of Zhengzhou University, Zhengzhou, Henan 450052, P.R. China

Received April 6, 2022; Accepted August 25, 2022

DOI: 10.3892/etm.2022.11623

Abstract. Brain death (BD) results in injury to organs and induces lung donor dysfunction. Since the 20S proteasome abnormality is associated with a variety of diseases, the present study investigated whether it was involved in lung injury following BD in rats, and the effects of the proteasome inhibitor MG132 on lung injury was also assessed. Rats were assigned to a BD group or a control sham group. The BD group of rats were sacrificed at different time points after BD. Administration of MG132 was performed intraperitoneally 30 min before BD. Arterial blood was drawn to measure the oxygenation index [partial artery pressure of oxygen (PaO_2)/fractional concentration of inspired oxygen (FiO_2)]. The right lung was used for staining with hematoxylin and eosin, immunohistochemistry, immunofluorescence, western blotting and RT-qPCR analysis. The left lung was used to measure the wet and dry weights. Rat alveolar macrophages (NR8383) were treated with MG132 and hypoxia/reoxygenation (H/R) and used for western blotting and flow cytometry. The PaO_2/FiO_2 ratio decreased after BD; the wet/dry weight ratio, histological lung injury score and protein expression of 20S proteasome β1 and inducible nitric oxide synthase (iNOS) gradually increased in rats after BD. Colocalization in the immunofluorescence between 20S proteasome β1 and iNOS was observed. MG132 treatment increased the PaO_2/FiO_2 ratio and decreased the wet/dry weight ratio, histological lung injury score and protein expression of 20S proteasome β1 and iNOS in rats after BD. MG132 was revealed to increase NR8383 apoptosis after H/R and to upregulate the protein expression levels of p-JNK and cleaved-caspase 3. Overall, the proteasome inhibitor MG132 could effectively reduce lung injury, which may be associated with its ability to inhibit the expression of the proteasome and promote the apoptosis of alveolar macrophages.

Correspondence to: Dr Shuijun Zhang, Department of Hepatobiliary and Pancreatic Surgery, The First Affiliated Hospital of Zhengzhou University, 1 Jianshe East Road, Erqi, Zhengzhou, Henan 450052, P.R. China
E-mail: zhangshuijun@zzu.edu.cn

Abbreviations: BD, brain death; H/R, hypoxia reoxygenation; H&E, hematoxylin and eosin; iNOS, inducible nitric oxide synthase; PaO_2, partial artery pressure of oxygen; FiO_2, fractional concentration of inspired oxygen

Key words: brain death, lung injury, 20S proteasome, MG132, alveolar macrophage

Introduction

Lung transplants are one of the most important methods of saving the lives of patients with end-stage lung disease (1). However, the shortage of donor lung organs limits the number of lung transplants performed (2). To reduce the gap between the number of lung donors and patients who require a transplant, several research centers have taken a series of measures, such as expanding donor standards and implementing extracorporeal lung perfusion after cardiac death (3). At present, the majority of donor lungs come from patients who have been declared brain-dead (4). Compared with other donor organs from who have been declared brain-dead, the utilization rate of lung donors is not high and there are regional differences in different countries (5-62%) (5-7). And the incidence rate of complications following lung transplantation, such as graft rejection, after brain death is higher compared with heart transplantation (33 vs. 17%) (8-10). Therefore, to improve the quality of donor lungs and reduce the number of complications after transplantation, there is a need to improve lung injury after brain death (BD).

A previous study has suggested that lung endoplasmic reticulum stress is involved in lung apoptosis during BD in rats (11). Endoplasmic reticulum stress is characterized by the accumulation of unfolded or misfolded proteins in the endoplasmic reticulum that can cause an unfolded protein response (UPR) and endoplasmic reticulum-associated degradation (ERAD) (12). This can escalate to involve the ubiquitin proteasome system (UPS), degrading ubiquitinated misfolded and unfolded proteins (13). Therefore UPR, ERAD and UPS interact in a coordinated manner to maintain the intracellular

protein balance (14). The most common proteasome in UPS, the 26S proteasome, is composed of the 20S proteasome and 19S regulatory particles, both of which participate in degrading ubiquitin-tagged proteins (15). The 20S proteasome has α and β subunits, and the 20S proteasome β subunits display chymotrypsin (β5)-, trypsin (β2)- and caspase (β1)-like activity (16). 20S proteasome dysfunction is involved in the pathophysiology of various acute and chronic lung diseases (17,18). Proteasome inhibitors can restore protein homeostasis, reduce oxidative stress and apoptosis and improve organ ischemia-reperfusion injury (19). Previous investigation has revealed their potential role in protection of kidney transplantation (20). However, information on the effect of the proteasome inhibitor on lung injury in brain-dead donors is sparse.

The aim of the current study was to explore whether the 20S proteasome was involved in lung injury after BD in rats, as well as the effect and mechanism of the proteasome inhibitor MG132 on this lung injury, to provide a potential new method to improve the lung donor function after BD.

Materials and methods

Experimental animals and groups. A total of 60 adult male Sprague Dawley rats, 2-4 months old, weighing 200-250 g, were housed at 22˚C, with a 12-h light/dark cycle, and with relative humidity maintained at 40-60% and with free access to food and water in the Henan Provincial Experimental Animal Center, Zhengzhou, China. The experimental protocols complied with the Guide for the Care and Use of Laboratory Animals of the National Institutes of Health (21).

Induction of BD. Animals were anesthetized with 1% pentobarbital sodium (60 mg/kg) by intraperitoneal injection (ip), and their arterial pressure was monitored via the femoral artery. Venous access was established through the femoral vein and the urine volume was monitored by cystostomy. The rats were intubated by tracheotomy mechanically, with an oxygen fraction of 100% (Harvard Apparatus). Next, a 2-mm hole was drilled with a marathon-3 dental grinder (Saeyang Co., Ltd.) through the skull, 4-mm lateral to the sagittal suture. Next, a 3F Fogarty Catheter (Edwards Lifesciences) was placed and inflated with 20 μl fluid every 5 min until BD was achieved (11). During the entire experimental procedure, SpO_2 remained >90% and the SBP remained ≥90 mmHg.

BD was confirmed by induction of a deep coma, spontaneous respiratory arrest, mydriasis, absence of brainstem reflexes and an amplitude of the electroencephalogram <0.02 v.

Animal groups. Animals were randomly assigned into the following groups: i) Sham operation group (sham, n=6); ii) BD groups (the BD subgroups were divided into BD 0.5, 1, 2, 4 and 6 h according to the time of specimen collection; n=6 per group); iii) MG132 groups, in which MG132 (cat. no. m1902; Abmole Bioscience Inc.) was dissolved in DMSO, diluted to 10 mmol/l with PBS and was administered at a dose of 10 mg/kg (ip) ~30 min before BD induction (22) (the MG132 subgroups were divided into BD 2 h + MG132 and BD 6 h + MG132; n=6 per group); and iv) control groups in which an equivalent volume of DMSO to that in the MG132 group 30 min before BD induction (the control subgroups were divided into BD 2 h + control and BD 6 h + control; n=6 per group).

Specimen collection. The blood was drawn from the femoral artery to measure partial artery pressure of oxygen (PaO_2). Rats were sacrificed by exsanguination of the abdominal aorta until cardiac arrest was achieved. The right lower lung was fixed with 4% paraformaldehyde at room temperature for 7 days, the right middle lung after removal was quickly placed in liquid nitrogen and then transferred to be frozen in a -80˚C refrigerator for the next experiments within 3 months and the weight of the left lung was measured (wet weight and dry weight after 1 week in a 60˚C oven). Bronchoalveolar lavage fluid (BALF) was obtained by lavage of the left main bronchus with 2 ml normal saline repeated three times after clipping the right main bronchus according to previous research methods (11). After mixing, 10 μl of BALF was collected into the cell counter (Jiangsu Jimbio Technology Co., Ltd.) to measure the cell concentration in BALF, and these data are displayed below. The BALF was centrifuged at 13,800 x g/min for 10 min at 4˚C, the cell sediment was resuspended with 500 μl normal saline to make cell smears to observe the cell morphology by using hematoxylin and eosin (H&E) staining as described below, and the supernatant was obtained to measure the protein concentration using a bicinchoninic acid assay.

H&E staining. The right lower lobe was fixed in 4% paraformaldehyde for 7 days at room temperature, embedded in paraffin, sectioned at 4-μm and stained with H&E staining (11). The paraffin sections were heated at 60˚C oven for 1 h, dewaxed twice in xylene solutions for 10 min each and rehydrated in descending alcohol series. The paraffin slides were stained with hematoxylin for 5 min at room temperature and differentiated with 0.1% hydrochloric acid ethanol for 1 min, followed with eosin for 5 min at room temperature, dehydrated in ascending alcohol series, followed by being dewaxed twice in xylene solutions for 10 min each. The cell smears were fixed with 95% alcohol for 10 min, and the following steps of staining were the same as those for paraffin sections. The slides were captured using a conventional light microscope (Axiolab 5; Zeiss GmbH) at a magnification of x200. A semiquantitative severity-based scoring system was used as previously described in the reference (23): i) Intra- and extra-alveolar hemorrhage; ii) intra-alveolar edema; iii) inflammatory infiltration of the inter-alveolar septa and airspace; iv) over-inflation; and v) erythrocyte accumulation below the pleura. Variables i) -iv) were graded as: 0=Negative, 1=slight, 2=moderate, 3=high and 4=severe. Variable v) was scored as 0=absent or 1=present. Lungs were scored by two blinded investigators, across 10 random, non-coincidental fields per section and then the mean values were analyzed.

Immunohistochemistry staining. The paraffin sections were heated at 60˚C oven for 1 h, dewaxed twice in xylene solutions for 15 min each and rehydrated in descending alcohol series. Antigen retrieval was performed with sodium citrate buffer (cat. no. C1031; Beijing Solarbio Science & Technology Co., Ltd. China) at 100˚C for 10 min. The slides were immersed in 3% H_2O_2 at room temperature for 30 min to inhibit endogenous peroxidase activity. The slides were then blocked with 10%

normal goat serum (cat. no. WGAR1009-5; Wuhan Servicebio Technology Co., Ltd.) at room temperature for 1 h. The slides were incubated with the primary antibody at 4˚C overnight followed with secondary antibody at room temperature for 1 h. The primary antibody used was a 20S proteasome β1 antibody (1:100 diluted in 1% BSA; cat. no. sc-374405; Santa Cruz Biotechnology, Inc.). The secondary antibody used was Biotin-conjugated Affinipure goat anti-mouse IgG (1:100; cat. no. SA00004-1; ProteinTech Group, Inc.). DAB was added for color development for 10 min and then counterstained with hematoxylin for 5 min at room temperature. Single sections from five rats per a group were evaluated. The slides were captured using a Nikon ECLIPSE Ni-E400 fluorescence microscope (Nikon Corporation). Semi-quantitative image analysis was performed by using the open-source software Image J 1.53e (National Institutes of Health) plugin the IHC profiler (24). The staining score was scored as 4 (high positive), 3 (positive), 2 (low positive) and 1 (negative); the staining positive number score was defined in at least five areas (x400 magnification per section) in a blinded manner and scored as 1 (<10%), 2 (10-49%), 3 (50-74%) and 4 (75-100%). The final score was defined as staining number score multiplied by staining color score as described before (25).

Immunofluorescence staining. Immunofluorescence staining was performed as described previously (26). The paraffin sections were heated at 60˚C oven for 1 h, washed twice in xylene solutions for 15 min each, rehydrated in descending alcohol series, blocked with sodium citrate buffer (cat. no. C1031; Beijing Solarbio Science & Technology Co., Ltd. China) at 100˚C for 10 min, incubated with primary antibodies for 6 h at 4˚C, followed by secondary antibodies for 6 h at 4˚C in an opaque wet box and stained with DAPI for 10 min at room temperature in the dark. The primary antibodies used were 20S proteasome β1 (1:100 diluted with 1% BSA; cat. no. sc-374405, Santa Cruz Biotechnology, Inc.) and inducible nitric oxide synthase (iNOS; 1:100; cat. no. GB11119; Wuhan Servicebio Technology Co., Ltd.), myeloperoxidase (MPO; 1:100; cat. no. GB11224; Wuhan Servicebio Technology Co., Ltd.) and CD31 (1:100; cat. no. GB113151; Wuhan Servicebio Technology Co., Ltd.). The secondary antibodies used were Cy3-conjugated Affinipure goat anti-rabbit IgG (1:100; cat. no. SA00009-2; ProteinTech Group, Inc.) or Coralite488-conjugated goat anti-mouse IgG (1:100; cat. no. SA00013-1; ProteinTech Group, Inc.). An Olympus fluorescence microscope (Olympus Corporation) was used to obtain images at excitation/emission wavelengths of 547/570 nm (Cy3, red), 494/520 nm (Coralite488, green), and 360/460 nm (DAPI, blue) (original magnification x400).

Reverse transcription-quantitative PCR (RT-qPCR). The mRNA levels of Psmb1 were measured using RT-qPCR. Total RNA was extracted from lung tissues using TRIzol® (Invitrogen; Thermo Fisher Scientific, Inc.), and reverse transcription was performed as described previously (27). Synthesis of cDNA and sample preparation were performed according to the manufacturer's instructions for the PrimeScript RT reagent kit (Takara Bio, Inc.) and SYBR Premix Ex Taq kit (Takara Bio, Inc.), respectively. qPCR was performed using a QuantStudio 5 Real-Time PCR System (Thermo Fisher Scientific, Inc.). The thermocycling conditions were 95˚C for 30 sec, 95˚C for 5 sec and 60˚C for 35 sec (40 cycles). The method of quantification ($2^{-\Delta\Delta Cq}$ method) was performed as described previously (28). The primer sequences (Invitrogen; Thermo Fisher Scientific, Inc.) used in this experiment are provided in Table SI.

Cell hypoxia/reoxygenation (H/R). Rat alveolar macrophages (NR8383 cell line; The Cell Bank of Type Culture Collection of The Chinese Academy of Sciences) have been demonstrated to closely mimic the important biological characteristics of normal alveolar macrophages previously, and have been used instead of primary alveolar macrophages (29,30). The cells were cultured in a semi-suspension with Ham's F-12 Nutrient Mixture (cat. no. GNM21700; Genom) supplemented with 20% FBS (cat. no. WGG8001-100; Wuhan Servicebio Technology Co., Ltd.) at 37˚C, in a humidified incubator supplied with 20% O_2 and 5% CO_2. NR8383 cells were serum starved for 6 h to ensure synchronization of the cell cycle and were pretreated with 10 μM MG132 (MG132 group) or an equivalent volume of DMSO vehicle (control group) for 1 h. The cells were then cultured in an incubator supplied with 1% oxygen for 2 h or 6 h to mimic hypoxia (30). Cells were then treated as follows: Half of the medium was absorbed, and the same amount of 40% FBS and medium along with the same drug concentration was added and reoxygenated in the normoxic incubator for 2 h.

Apoptosis analysis of NR8383 cells using flow cytometry. A total of $1x10^6$ cells/ml NR8383 cells were prepared according to the instructions of the Annexin V-FITC/PI Apoptosis Detection kit (cat. no. ca1020; Beijing Solarbio Science & Technology Co., Ltd.). Briefly, NR8383 cells were harvested and resuspended with 100 μl binding buffer. Cells were incubated with 5 μl Annexin V-FITC at room temperature for 5 min in the dark, then 5 μl PI and 400 μl of PBS were added. Apoptosis was detected using a flow cytometry (BD FACSCantoII; BD Biosciences) and analyzed using BD FACSDiva Software v8.0.1 (BD Biosciences).

Western blotting. The proteins were extracted from lung tissue or cells and lysed by using RIPA buffer (high; cat. no. R0010; Beijing Solarbio Science & Technology Co., Ltd.) on ice for >30 min. Protein levels were quantified using BCA reagent. Samples were loaded 10 μl per lane and electrophoresed by 10% SDS-PAGE and transferred to polyvinylidene difluoride membranes. The membranes were blocked in 5% non-fat milk for 2 h at room temperature. The membranes were incubated with primary antibodies at 4˚C overnight. The primary antibodies used were: 20S proteasome β1 (1:500; cat. no. sc-374405; Santa Cruz Biotechnology, Inc.), iNOS (1:1,000; cat. no. AF0199; Affinity Biosciences), cleaved caspase 3 (1:1,000; cat. no. 9661; Cell Signaling Technology, Inc.), p-JNK (1:1,000; cat. no. ET1609-42; HUABIO, Inc.), total JNK Antibody (1:500; cat. no. ET1601-28; HUABIO, Inc.) and GAPDH (1:5,000; cat. no. 60004-1-lg; ProteinTech Group, Inc.). The secondary antibodies used were horseradish peroxide-conjugated goat anti-mouse IgG (1:5,000; cat. no. SA00001-1; ProteinTech Group, Inc.) and goat anti-rabbit IgG (1:5,000; cat. no. SA00001-2; ProteinTech Group, Inc.). The bands were visualized using the Chemiluminescent Substrate kit (cat. no. PE0010; Beijing Solarbio Science & Technology

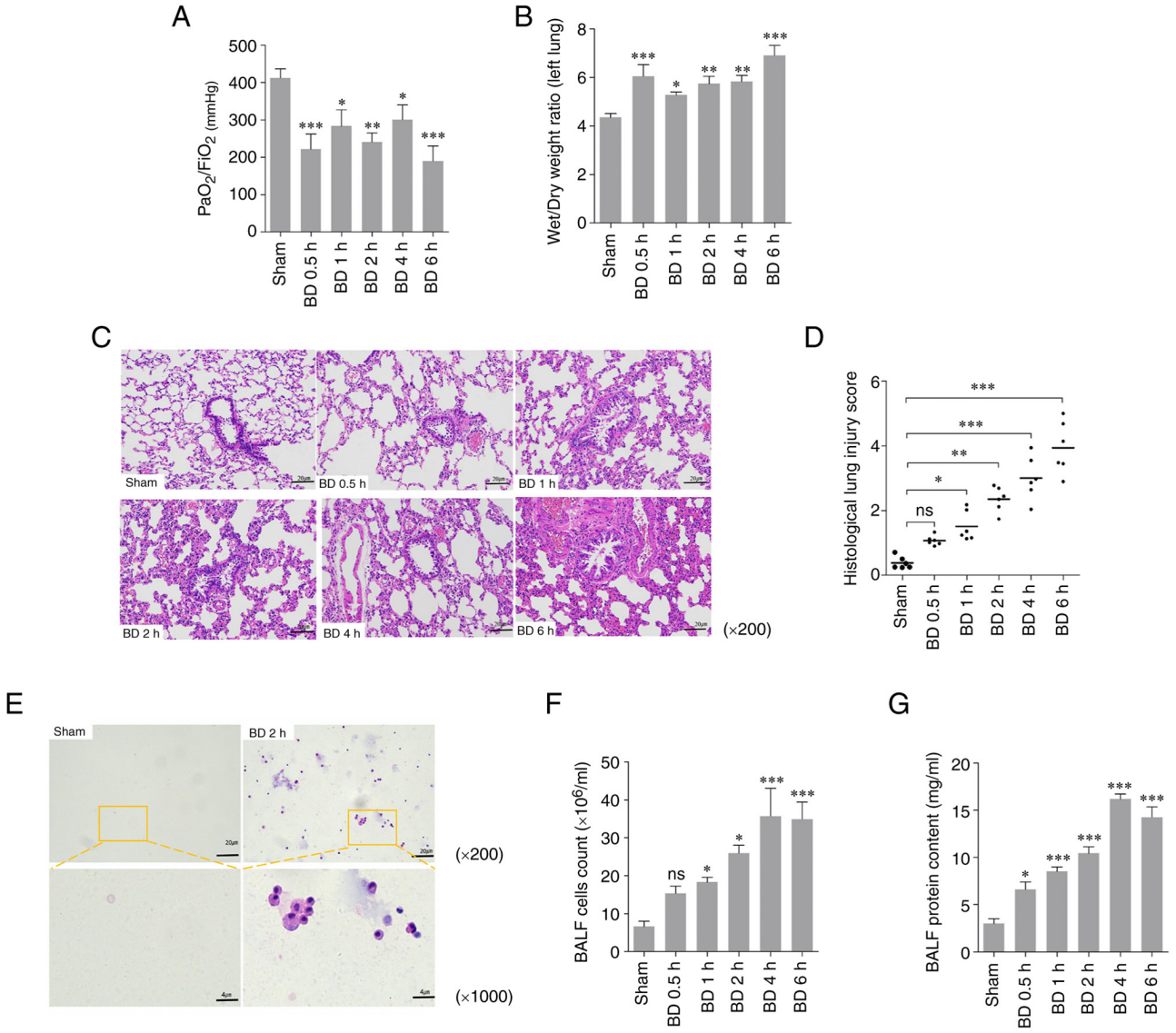

Figure 1. Lung injury after BD in rats. (A) PaO_2/FiO_2 (mmHg) ratio in the rats amongst the different groups. (B) Wet/dry weight ratio of the left lung in the rats amongst the different groups. (C) Histopathological sections of H&E staining (original magnification x200) and (D) the histological lung injury score evaluated through H&E staining in the rats amongst the different groups as median and range. (E) Cells in the BALF in the rats amongst the different groups (original magnification: Top row, x,200; bottom row, x1,000). (F) Cell count and (G) the protein content in BALF amongst the different groups. *P<0.05, **P<0.01 and ***P<0.001 vs. sham. ns/no significance; BD, brain death; PaO_2, partial artery pressure of oxygen; FiO_2, fractional concentration of inspired oxygen; H&E, hematoxylin and eosin; BALF, bronchoalveolar lavage fluid.

Co., Ltd.) combined with a Bio-Rad exposure system (Bio-Rad Laboratories, Inc.) and analyzed using ImageJ 1.53e.

Statistical analysis. All experiments were repeated three times. Statistical analysis was performed using GraphPad Prism version 5.0 (GraphPad Software, Inc.). The ordinal data (hispathological injury scores, IHC scores) are presented as median and range, and differences between sham group and BD groups were analyzed using the Kruskal-Wallis test followed by Dunn post hoc tests. Other data are presented as the mean ± SD, and differences in characters [PaO_2/fractional concentration of inspired oxygen (FiO_2), Wet/Dry weight ratio of left lung, BALF cells count, BALF protein content, relative protein level, relative expression of Psmb1) between sham group and BD groups were analyzed using a one-way ANOVA followed by Bonferroni's test in the post-hoc comparison. Differences in other characters between control groups and MG132 groups were analyzed using a one-way ANOVA followed by unpaired Student's t-test. P<0.05 was considered to indicate a statistically significant difference.

Results

Lung injury gradually increases in rats following BD. To evaluate the lung injury after BD in rats, the oxygenation index (PaO_2/FiO_2), the wet/dry weight ratio, H&E staining, and histological lung injury scores were used to evaluate the standard of lung injury in lung tissue at different time points after BD. The PaO_2/FiO_2 of the BD groups were significantly lower compared with that of the sham group (Fig. 1A). The wet/dry weight ratios of the left lung in the BD groups were significantly higher compared with that of the sham group

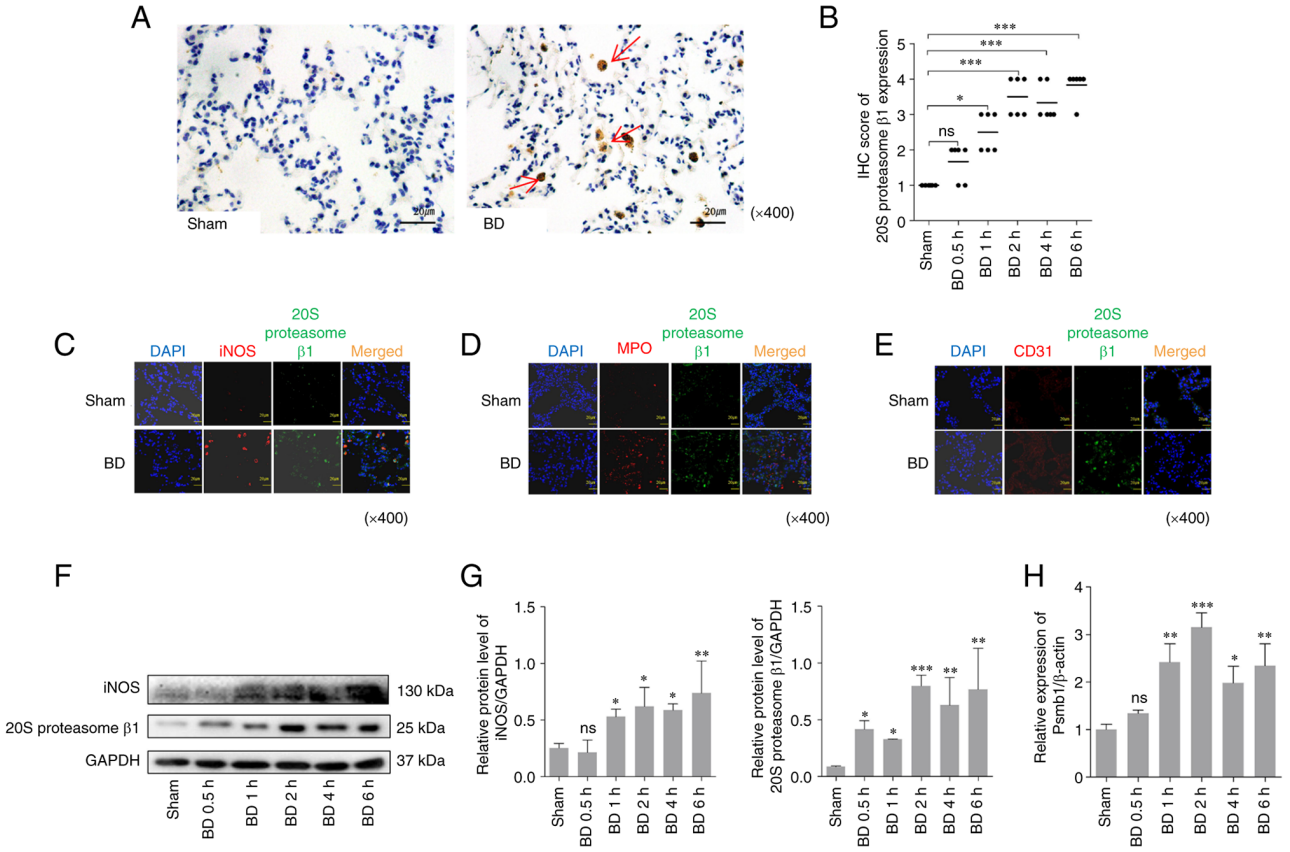

Figure 2. Expression of the 20S proteasome β1 in lung tissues after BD in rats. (A) IHC staining of the 20S proteasome β1 in lung tissues 2 h after BD and in the sham group (original magnification x400). The arrows show the 20S proteasome β1 positive cells. (B) Semi-quantitative evaluation of 20S proteasome IHC staining in lung tissues amongst the different groups. (C-E) Immunofluorescence expression of 20S proteasome β1 and (C) iNOS, (D) MPO and (E) CD31 in lung tissues 2 h after BD and in the sham group (original magnification x400). Green, 20S proteasome β1; red, iNOS/MPO/CD31; orange, merged expression showing colocalization. (F) Western blotting and (G) quantification of the protein expression levels of the 20S proteasome β1 and iNOS from extracts of the lung tissue amongst the different groups. (H) Relative Psmb1 levels in lung tissues after BD detected by RT-qPCR. *P<0.05, **P<0.01, ***P<0.001 vs. sham. ns/no significance; BD, brain death; IHC, immunohistochemistry; iNOS, inducible nitric oxide synthase; MPO, myeloperoxidase.

(Fig. 1B). Compared with the sham group, pulmonary alveolar wall thickening, pulmonary hemorrhage, and neutrophil infiltration were observed in the BD rats (Fig. 1C); the histological lung injury scores increased over time and were significantly higher compared with that in the sham group (Fig. 1D). Based on the microscopic images, a notable increase in the proportion of cells in the BALF was observed (Fig. 1E). The cell count and the protein content in the BALF was higher in the experimental group compared with that in the sham group (Fig. 1F and G). These results indicated that lung injury gradually increased in rats after BD.

Expression of the 20S proteasome β1 is increased in the lung tissues of BD rats. The 20S proteasome β1 is a subunit of the 20S proteasome with caspase-like activity that is inhibited by MG132 (31). Immunohistochemical semi-quantitative analysis, western blotting and RT-qPCR were used to detect the expression of the 20S proteasome β1. As presented in Fig. 2, induction of BD significantly increased the expression of the 20S proteasome β1 in the lung tissues compared with the sham group (Fig. 2A, B, F and G).

Notably, the 20S proteasome β1 positive cells exhibited an alveolar macrophage-like morphology. To confirm the upregulation of the 20S proteasome β1 in alveolar cells from the lung tissues following BD, immunofluorescence staining was used to detect the co-localization of 20S proteasome β1 and iNOS/MPO/CD31 in lung tissue sections of rats after BD (MPO is considered as one of markers of neutrophil activation, CD31 is one of the markers of endothelial cell and iNOS is considered one of the markers of macrophages). The results indicated the presence and the differences in the co-localization of the 20S proteasome β1 and iNOS/MPO/CD31 in the lung tissues, and 20S proteasome β1 mostly colocalized with iNOS, but not with MPO and CD31 (Fig. 2C-E) to rule out the increased high expression of 20S proteasome β1 on neutrophils/endothelial cells. Compared with the sham group, induction of BD significantly increased the protein expression of the 20S proteasome β1 and iNOS (Fig. 2F and G) and also increased the relative Psmb1 levels (Fig. 2H).

Inhibition of the proteasome by MG132 reduces lung injury following BD. To explore the effect of proteasomal inhibition on lung injury following BD in rats, a proteasome inhibitor, MG132, was administered before induction of BD and the specimens were collected for analysis at different time points following BD. Compared with the control group, MG132 treatment was revealed to significantly increase the PaO_2/FiO_2 after BD (Fig. 3A) and significantly reduce the left lung

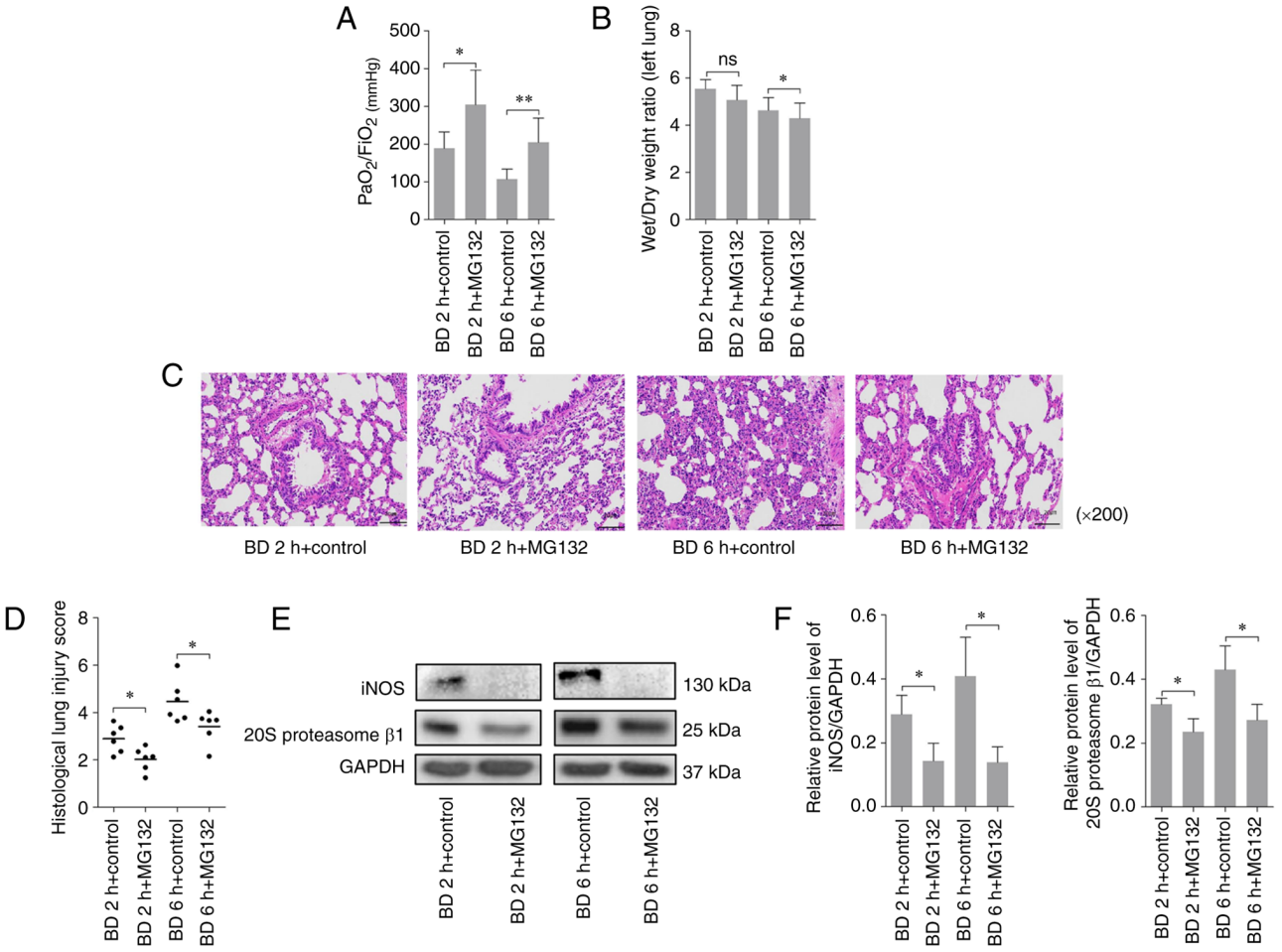

Figure 3. Effect of MG132 on lung injury after BD. (A) PaO_2/FiO_2 (mmHg) ratio in the rats amongst the different groups. (B) Wet/dry weight ratio of the left lung in the rats amongst the different groups. (C) Histopathological sections of H&E staining (original magnification x200) and (D) the histological score of lung injury evaluated through H&E staining in the rats amongst the different groups. (E) Western blotting and (F) quantification of the protein expression levels of the 20S proteasome β1 and iNOS from extracts of the lung tissue amongst the different groups. $^{*}P<0.05$, $^{**}P<0.01$. ns/no significance; BD, brain death; PaO_2, partial artery pressure of oxygen; FiO_2, fractional concentration of inspired oxygen; iNOS, inducible nitric oxide synthase.

wet/dry weight ratio 6 h after BD (Fig. 3B). However, MG132 treatment also alleviated the thickening of the alveolar wall, pulmonary hemorrhage, and neutrophil infiltration (Fig. 3C), whilst also significantly decreasing the histological lung injury scores compared with the control group (Fig. 3D). As presented in Fig. 3E and F, MG132 treatment significantly reduced the protein expression levels of the 20S proteasome β1 and iNOS in lung tissues following BD at 2 and 6 h. These results suggested that inhibition of the proteasome by MG132 decreased lung injury after BD.

MG132 increases apoptosis following H/R in cultured rat alveolar macrophages. Previous studies suggest that in the acute stage of infection or BD, alveolar macrophages are rapidly recruited and they secrete a large quantity of harmful substances, which in turn attack the lung tissues and induce lung tissue injury (32,33). As the upregulation of 20S proteasome β1 in alveolar macrophages was confirmed, whether MG132 treatment protected lung tissues via induction of apoptosis of alveolar macrophages was next assessed. To test this hypothesis, NR83883 cells (rat alveolar macrophage cells) were used as an *in vitro* model. Flow cytometry and western blotting were used to detect the apoptosis of NR8383 cells after hypoxia treatment for 2 or 6 h, followed by re-oxygenation for 2 h. Compared with the control group, MG132 treatment significantly increased the apoptotic rate of NR8383 cells (Fig. 4A and B) after 2 h of hypoxia and 2 h of re-oxygenation (H/R-2/2), and after 6 h of hypoxia and 2 h of re-oxygenation (H/R-6/2). In addition, MG132 administration significantly increased the protein expression levels of p-JNK and cleaved-caspase 3 in NR8383 cells after H/R-2/2 and H/R-6/2 compared with the control group (Fig. 4C and D). These results highlighted that inhibition of proteasomal activity using MG132 increased cell apoptosis after H/R in cultured rat alveolar macrophages.

Discussion

BD can lead to a series of pathophysiological changes, including hemodynamic, metabolomic, inflammatory and neuroendocrinal abnormalities (34). All of these can contribute to lung injury. The donor lung after BD is associated with a high incidence rate of complications following lung transplantation (8-10). Thus, there is a need to study the mechanism of lung injury after BD and to develop effective therapeutics to decrease lung injury.

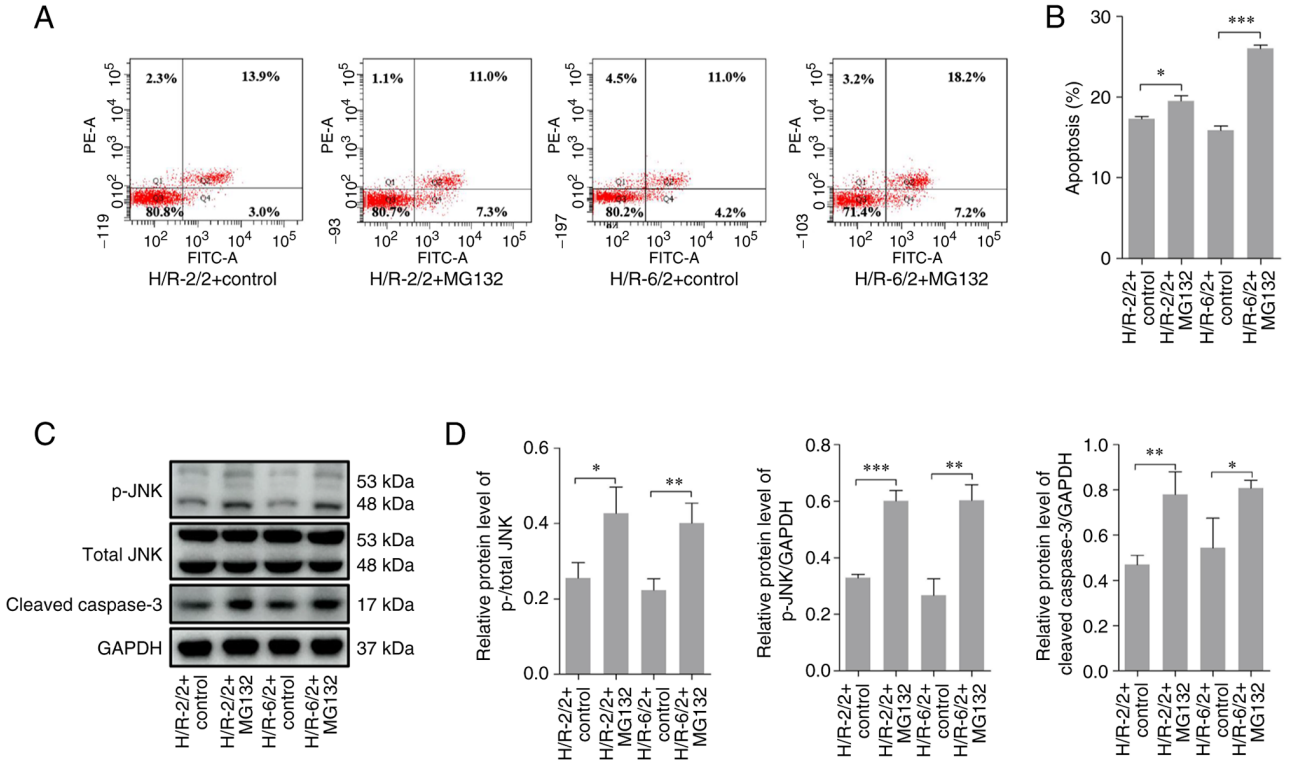

Figure 4. Effect of MG132 on apoptosis of NR8383 cells after H/R. (A) Apoptosis of NR8383 cells pretreated with the vehicle control (DMSO) or MG132 (10 μM) based on flow cytometry and (B) the quantified apoptotic rates. (C) Western blotting and (D) quantification of the protein levels of p-JNK and cleaved-caspase 3 in NR8383 cell extracts from the control group and MG132 group after H/R-2/2 and H/R-6/2. (All experiments were performed using the same protein extract, but due to the molecular weights of the target protein and the loading control protein being close, not all proteins were probed on the same membrane, but all experiments were performed as a single batch under identical conditions). *P<0.05, **P<0.01 and ***P<0.001. H/R, hypoxia/reoxygenation; H/R-2/2, hypoxia for 2 h then reoxygenation for 2 h; H/R-6/2, hypoxia for 6 h then reoxygenation for 2 h; p-, phosphorylated.

In the present study, a decrease in the arterial oxygenation index and an increase in the left lung wet/dry weight ratio and the aggravation of lung pathological injury were observed after BD in rats, in accordance with published results describing the lung after BD (35,36).

The UPS is an important pathway for maintaining protein homeostasis in eukaryotic cells (37). The 20S proteasome β1 subunit is a component of the 26S proteasome (15,16). The biological activity of the 20S proteasome can be detected in the alveolar space of patients with acute lung injury (17). In addition, the protein concentration of the 20S proteasome is also significantly increased in the alveolar space of patients with acute lung injury and in the circulation of patients with sepsis (38). In agreement with the previous data, in the present study the expression of the 20S proteasome increased over time in the lung tissues of rats after BD compared with the sham group samples. These results suggested that the 20S proteasome was involved in lung injury after BD.

The present results demonstrated that MG132, as a proteasome inhibitor, improved the arterial blood oxygenation index, alleviated lung pathological manifestations and reduced the left lung wet/dry weight ratio in rats after BD, suggesting that MG132 could decrease lung injury after BD in rats. In addition, MG132 was revealed to downregulate the protein expression levels of the 20S proteasome β1 subunit at the same time. It has previously been demonstrated that MG132 can decrease the levels of inflammatory cytokines in BALF in a model of sepsis-induced acute lung injury, suggesting that MG132 crosses the blood-air barrier and gains access to lumen facing cells such as the alveolar macrophages (39,40). Therefore, it was speculated that that MG132 may play a role in lung protection by inhibiting the expression of the proteasome.

The current study revealed that the 20S proteasome β1 and iNOS were colocalized in lung tissues after BD using an immunofluorescence assay and the protein expression levels were also significantly augmented in lung tissues following BD. Previous studies have detected iNOS expression in lung tissues after BD and reveal that in response to inflammatory stimuli, activated alveolar macrophages express high levels of iNOS and produce large amounts of NO, eventually resulting in tissue damage (41,42). Alveolar macrophages in the lungs express iNOS and are important sources of endogenous pulmonary NO production in inflammatory states, such as septic ALI (43-45).

MG132 treatment can inhibit the protein expression of iNOS through inhibition of the JNK/c-Myc signaling pathway and plays a protective role in sepsis-induced ALI (46). The current study demonstrated that MG132 treatment could inhibit the protein expression of 20S proteasome β1 and iNOS in lung tissues following BD in rats, indicating that the effect of MG132 treatment may be associated with alveolar macrophages. The NR8383 cell line has been demonstrated to closely mimic important biological characteristics of normal alveolar macrophages (47); thus, it was selected in the current study as a model cell hypoxia reoxygenation model for a cell experiment, which revealed that MG132 could promote the cell death of rat alveolar macrophages after H/R injury.

In addition, MG132 acts as a proteasome inhibitor, primarily affecting the caspase-related pathways (30). The JNK signal transduction pathway is an important member of the MARK pathway, which mediates intracellular signal transduction and induces apoptosis by activating the caspase family protein kinase (48). Previous studies have indicated that MG132 can promote the activity of JNKs49,50). The current study revealed that MG132 upregulated p-JNK protein expression and activated caspase 3, which promoted NR8383 apoptosis after H/R. Therefore, it is speculated that MG132 may promote the apoptosis of rat alveolar macrophages by mediating the JNK-caspase pathway, thus protecting the lungs after BD.

In conclusion, the 20S proteasome was demonstrated to be involved in lung injury after BD in rats, and MG132 could effectively reduce lung injury. This may be associated with the ability of MG132 to inhibit the expression of the proteasome in lung tissues and promote the apoptosis of alveolar macrophages. As such, this drug should be further explored regarding its potential to protect potential donor lungs following BD.

Acknowledgements

We would like to thank Dr H.W. Tang (Henan Key Laboratory of Digestive Organ Transplantation, First Affiliated Hospital of Zhengzhou University, Zhengzhou, China) for their technical assistance.

Funding

This study was supported by the National Natural Science Foundation of China (grant no. 81971881).

Availability of data and materials

All data generated or analyzed during this study are included in this published article.

Authors' contributions

HS, DY, and ZH performed the experiments. YL and HS performed the literature search and analyzed the data. WG and SZ interpreted the data. SZ, WG and HS designed the study. HS, DY and YL prepared and wrote the study. HS and SZ confirm the authenticity of all the raw data. All authors have read and approved the final manuscript.

Ethics approval and consent to participate

The protocol used in the present study was approved by the Institutional Animal Care and Use Committee of Zhengzhou University (approval no. 2019-ky-019).

Patient consent for publication

Not applicable.

Competing interests

The authors declare that they have no competing interests.

References

1. Nathan SD: The future of lung transplantation. Chest 147: 309-316, 2015.
2. Young KA and Dilling DF: The Future of Lung Transplantation. Chest 155: 465-473, 2019.
3. Jin Z, Hana Z, Alam A, Rajalingam S, Abayalingam M, Wang Z and Ma D: Review 1: Lung transplant-from donor selection to graft preparation. J Anesth 34: 561-574, 2020.
4. Van Raemdonck D, Keshavjee S, Levvey B, Cherikh WS, Snell G, Erasmus M, Simon A, Glanville AR, Clark S, D'Ovidio F, *et al*: Donation after circulatory death in lung transplantation-five-year follow-up from ISHLT Registry. J Heart Lung Transplant 38: 1235-1245, 2019.
5. Kute V, Ramesh V, Shroff S, Guleria S and Prakash J: Deceased-Donor organ transplantation in India: Current status, challenges, and solutions. Exp Clin Transplant 18 (Suppl 2): S31-S42, 2020.
6. Yeo HJ, Yoon SH, Lee SE, Jeon D, Kim YS, Cho WH and Kim DH: Current status and future of lung donation in Korea. J Korean Med Sci 32: 1953-1958, 2017.
7. Paraskeva MA, Levin KC, Westall GP and Snell GI: Lung transplantation in Australia, 1986-2018: More than 30 years in the making. Med J Aust 208: 445-450, 2018.
8. Ware LB, Wang Y, Fang X, Warnock M, Sakuma T, Hall TS and Matthay M: Assessment of lungs rejected for transplantation and implications for donor selection. Lancet 360: 619-620, 2002.
9. Zweers N, Petersen AH, van der Hoeven JA, de Haan A, Ploeg RJ, de Leij LF and Prop J: Donor brain death aggravates chronic rejection after lung transplantation in rats. Transplantation 78: 1251-1258, 2004.
10. Takahashi T, Terada Y, Pasque MK, Itoh A, Nava RG, Puri V, Kreisel D, Patterson AG and Hachem RR: Comparison of outcomes in lung and heart transplant recipients from the same multiorgan donor. Clin Transplant 34: e13768, 2020.
11. Tang H, Zhang J, Cao S, Yan B, Fang H, Zhang H, Guo W and Zhang S: Inhibition of endoplasmic reticulum stress alleviates lung injury induced by brain death. Inflammation 40: 1664-1671, 2017.
12. Hwang J and Qi L: Quality control in the endoplasmic reticulum: Crosstalk between ERAD and UPR pathways. Trends Biochem Sci 43: 593-605, 2018.
13. Xia SW, Wang ZM, Sun SM, Su Y, Li ZH, Shao JJ, Tan SZ, Chen AP, Wang SJ, Zhang ZL, *et al*: Endoplasmic reticulum stress and protein degradation in chronic liver disease. Pharmacol Res 161: 105218, 2020.
14. Cybulsky AV: The intersecting roles of endoplasmic reticulum stress, ubiquitin-proteasome system, and autophagy in the pathogenesis of proteinuric kidney disease. Kidney Int 84: 25-33, 2013.
15. Kopp F, Hendil KB, Dahlmann B, Kristensen P, Sobek A and Uerkvitz W: Subunit arrangement in the human 20S proteasome. Proc Natl Acad Sci USA 94: 2939-2944, 1997.
16. Everly JJ, Walsh RC, Alloway RR and Woodle ES: Proteasome inhibition for antibody-mediated rejection. Curr Opin Organ Transplant 14: 662-666, 2009.
17. Kerrin A, Weldon S, Chung AH, Craig T, Simpson AJ, O'Kane CM, McAuley DF and Taggart CC: Proteolytic cleavage of elafin by 20S proteasome may contribute to inflammation in acute lung injury. Thorax 68: 315-321, 2013.
18. Semren N, Welk V, Korfei M, Keller IE, Fernandez IE, Adler H, Günther A, Eickelberg O and Meiners S: Regulation of 26S proteasome activity in pulmonary fibrosis. Am J Respir Crit Care Med 192: 1089-1101, 2015.
19. Kukan M: Emerging roles of proteasomes in ischemia-reperfusion injury of organs. J Physiol Pharmacol 55 (1 Pt 1): 3-15, 2004.
20. Lo S, MacMillan-Crow LA and Parajuli N: Renal cold storage followed by transplantation impairs proteasome function and mitochondrial protein homeostasis. Am J Physiol Renal Physiol 316: F42-F53, 2019.
21. National Research Council (US), Committee for the Update of the Guide for the Care and Use of Laboratory Animals: Guide for the Care and Use of Laboratory Animals. 8th edition. National Academies Press (US),Washington, DC, 2011.
22. Chen X, Li SL, Wu T and Liu JD: Proteasome inhibitor ameliorates severe acute pancreatitis and associated lung injury of rats. World J Gastroenterol 14: 3249-3253, 2008.
23. van Zanden JE, Rebolledo RA, Hoeksma D, Bubberman JM, Burgerhof JG, Breedijk A, Yard BA, Erasmus ME, Leuvenink HGD and Hottenrott MC: Rat donor lung quality deteriorates more after fast than slow brain death induction. PLoS One 15: e242827, 2020.

24. Varghese F, Bukhari AB, Malhotra R and De A: IHC Profiler: An open source plugin for the quantitative evaluation and automated scoring of immunohistochemistry images of human tissue samples. PLoS One 9: e96801, 2014.
25. Guo Z, Zhang X, Zhu H, Zhong N, Luo X, Zhang Y, Tu F, Zhong J, Wang X, He J and Huang L: TELO2 induced progression of colorectal cancer by binding with RICTOR through mTORC2. Oncol Rep 45: 523-534, 2021.
26. Lee HY and Oh SH: Autophagy-mediated cytoplasmic accumulation of p53 leads to apoptosis through DRAM-BAX in cadmium-exposed human proximal tubular cells. Biochem Biophys Res Commun 534: 128-133, 2021.
27. Chen S, Fang H, Li J, Shi J, Zhang J, Wen P, Wang Z, Yang H, Cao S, Zhang H, *et al*: Microarray analysis for expression profiles of lncRNAs and circRNAs in rat liver after brain-dead donor liver transplantation. Biomed Res Int 2019: 5604843, 2019.
28. Livak KJ and Schmittgen TD: Analysis of relative gene expression data using real-time quantitative PCR and the 2(-Delta Delta C(T)) method. Methods 25: 402-408, 2001.
29. Hino M, Oda M, Yoshida A, Nakata K, Kohchi C, Nishizawa T, Inagawa H, Hori H, Makino K, Terada H and Soma G: Establishment of an in vitro model using NR8383 cells and Mycobacterium bovis Calmette-Guerin that mimics a chronic infection of Mycobacterium tuberculosis. In Vivo 19: 821-830, 2005.
30. Fan T, Huang Z, Wang W, Zhang B, Xu Y, Mao Z, Chen L, Hu H and Geng Q: Proteasome inhibition promotes autophagy and protects from endoplasmic reticulum stress in rat alveolar macrophages exposed to hypoxia-reoxygenation injury. J Cell Physiol 233: 6748-6758, 2018.
31. Kisselev AF: Site-Specific proteasome inhibitors. Biomolecules 12: 54, 2021.
32. Sutherland AJ, Ware RS, Winterford C and Fraser JF: The endothelin axis and gelatinase activity in alveolar macrophages after brain-stem death injury: A pilot study. J Heart Lung Transplant 26: 1040-1047, 2007.
33. Brieland JK, Kunkel RG and Fantone JC: Pulmonary alveolar macrophage function during acute inflammatory lung injury. Am Rev Respir Dis 135: 1300-1306, 1987.
34. Avlonitis VS, Fisher AJ, Kirby JA and Dark JH: Pulmonary transplantation: The role of brain death in donor lung injury. Transplantation 75: 1928-1933, 2003.
35. Sammani S, Park KS, Zaidi SR, Mathew B, Wang T, Huang Y, Zhou T, Lussier YA, Husain AN, Moreno-Vinasco L, *et al*: A sphingosine 1-phosphate 1 receptor agonist modulates brain death-induced neurogenic pulmonary injury. Am J Respir Cell Mol Biol 45: 1022-1027, 2011.
36. Wauters S, Somers J, De Vleeschauwer S, Verbeken E, Verleden GM, van Loon J and Van Raemdonck DE: Evaluating lung injury at increasing time intervals in a murine brain death model. J Surg Res 183: 419-426, 2013.
37. Goldberg AL: Protein degradation and protection against misfolded or damaged proteins. Nature 426: 895-899, 2003.
38. Roth GA, Moser B, Krenn C, Roth-Walter F, Hetz H, Richter S, Brunner M, Jensen-Jarolim E, Wolner E, Hoetzenecker K, *et al*: Heightened levels of circulating 20S proteasome in critically ill patients. Eur J Clin Invest 35: 399-403, 2005.
39. Wu B, Miao X, Ye J and Pu X: The protective effects of protease inhibitor MG-132 on sepsis-induced acute lung rats and its possible mechanisms. Med Sci Monit 25: 5690-5699, 2019.
40. Caldeira MV, Salazar IL, Curcio M, Canzoniero LM and Duarte CB: Role of the ubiquitin-proteasome system in brain ischemia: Friend or foe? Prog Neurobiol 112: 50-69, 2014.
41. Vieira RF, Breithaupt-Faloppa AC, Matsubara BC, Rodrigues G, Sanches MP, Armstrong-Jr R, Ferreira SG, Correia CJ, Moreira LFP and Sannomiya P: 17β-Estradiol protects against lung injuries after brain death in male rats. J Heart Lung Transplant 37: 1381-1387, 2018.
42. Forstermann U and Sessa WC: Nitric oxide synthases: Regulation and function. Eur Heart J 33: 829-837, 837a-837d, 2012.
43. Kobzik L, Bredt DS, Lowenstein CJ, Drazen J, Gaston B, Sugarbaker D and Stamler JS: Nitric oxide synthase in human and rat lung: Immunocytochemical and histochemical localization. Am J Respir Cell Mol Biol 9: 371-377, 1993.
44. Farley KS, Wang LF, Razavi HM, Law C, Rohan M, McCormack DG and Mehta S: Effects of macrophage inducible nitric oxide synthase in murine septic lung injury. Am J Physiol Lung Cell Mol Physiol 290: L1164-L1172, 2006.
45. Fujii Y, Goldberg P and Hussain SN: Contribution of macrophages to pulmonary nitric oxide production in septic shock. Am J Respir Crit Care Med 157 (5 Pt 1): 1645-1651, 1998.
46. Zhang Y, Huang T, Jiang L, Gao J, Yu D, Ge Y and Lin S: MCP-induced protein 1 attenuates sepsis-induced acute lung injury by modulating macrophage polarization via the JNK/c-Myc pathway. Int Immunopharmacol 75: 105741, 2019.
47. Helmke RJ, German VF and Mangos JA: A continuous alveolar macrophage cell line: Comparisons with freshly derived alveolar macrophages. In Vitro Cell Dev Biol 25: 44-48, 1989.
48. Bogoyevitch MA and Kobe B: Uses for JNK: The many and varied substrates of the c-Jun N-terminal kinases. Microbiol Mol Biol Rev 70: 1061-1095, 2006.
49. Wu HM, Wen HC and Lin WW: Proteasome inhibitors stimulate interleukin-8 expression via Ras and apoptosis signal-regulating kinase-dependent extracellular signal-related kinase and c-Jun N-terminal kinase activation. Am J Respir Cell Mol Biol 27: 234-243, 2002.
50. Tarjanyi O, Haerer J, Vecsernyes M, Berta G, Stayer-Harci A, Balogh B, Farkas K, Boldizsár F, Szeberényi J and Sétáló G Jr: Prolonged treatment with the proteasome inhibitor MG-132 induces apoptosis in PC12 rat pheochromocytoma cells. Sci Rep 12: 5808, 2022.